Complexity in subnetworks of a peroxidase–oxidase reaction model

Jason A. C. Gallas and Lars F. Olsen

View Online   Export Citation   CrossMark

Complexity in subnetworks of a peroxidase–oxidase reaction model

Jason A. C. Gallas[1,2,a)] (ID) and Lars F. Olsen[3,b)] (ID)

AFFILIATIONS

[1] Instituto de Altos Estudos da Paraíba, Rua Silvino Lopes 419-2502, 58039-190 João Pessoa, Brazil
[2] Max-Planck Institute for the Physics of Complex Systems, Nöthnitzer Str. 38, 01187 Dresden, Germany
[3] PhyLife, Institute of Biochemistry and Molecular Biology, University of Southern Denmark, DK-5230 Odense M, Denmark

Note: This article is part of the Focus Issue, From Chemical Oscillations to Applications of Nonlinear Dynamics Dedicated to Richard J. Field on the Occasion of his 80th Birthday.
[a)] **Also at:** Complexity Sciences Center, 9225 Collins Avenue Suite 1208, Surfside, Florida 33154-3001, USA.
Electronic mail: jason.gallas@gmail.com
[b)] **Author to whom correspondence should be addressed:** lfo@bmb.sdu.dk

ABSTRACT

The peroxidase–oxidase (PO) reaction is a paradigmatic (bio)chemical system well suited to study the organization and stability of self-sustained oscillatory phases typically present in nonlinear systems. The PO reaction can be simulated by the state-of-the-art Bronnikova–Fedkina–Schaffer–Olsen model involving ten coupled ordinary differential equations. The complex and dynamically rich distribution of self-sustained oscillatory stability phases of this model was recently investigated in detail. However, would it be possible to understand aspects of such a complex model using much simpler models? Here, we investigate stability phases predicted by three simple four-variable subnetworks derived from the complete model. While stability diagrams for such subnetworks are found to be distorted compared to those of the complete model, we find them to surprisingly preserve significant features of the original model as well as from the experimental system, e.g., period-doubling and period-adding scenarios. In addition, return maps obtained from the subnetworks look very similar to maps obtained in the experimental system under different conditions. Finally, two of the three subnetwork models are found to exhibit *quint points*, i.e., recently reported singular points where five distinct stability phases coalesce. We also provide experimental evidence that such quint points are present in the PO reaction.

Published under an exclusive license by AIP Publishing. https://doi.org/10.1063/5.0093169

The peroxidase–oxidase (PO) reaction is one of the simplest biological systems to exhibit complex dynamics. The reaction involves a single enzyme and two substrates plus one or two modifiers. The complex dynamics has been simulated by a realistic ten-variable mathematical model, the so-called Bronnikova–Fedkina–Schaffer–Olsen (BFSO) model. However, this model is by itself a complex system to analyze, so it would be convenient to break it up into smaller subnetworks that can be analyzed individually much more easily. Here, we study three simple four-variable subnetwork models derived from the full model. These three simpler models were previously introduced by Sensse, Hauser, and Eiswirth in an investigation of Shilnikov chaos in the PO reaction. We find that each of the three subnetwork models can well reproduce different aspects of the experimental system in terms of bifurcations and return maps. In addition, two of the models predict the existence of quint points, namely, very recently reported singular points where five distinct stability phases coalesce. New experimental data indicate that such quint points are indeed present in the experimental system.

I. INTRODUCTION

Complex dynamics is a widespread phenomenon in biological systems, ranging from the ten year oscillations observed in populations of Canadian lynx[1] to the fast complex oscillations in the electrical activity of the brain and the heart[2] to complex oscillations in intracellular concentration of calcium.[3] On a scale of even higher spatial resolution, one finds oscillations in enzyme catalyzed

---

reactions.[4,5] In this latter category, one also finds the oscillating peroxidase–oxidase reaction.[6]

The peroxidase–oxidase (PO) reaction entails the oxidation of an organic electron donor (YH_2) with molecular oxygen as the electron acceptor,

$$2YH_2 + O_2 \rightarrow 2Y + 2H_2O. \tag{1}$$
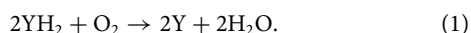
The reaction is catalyzed by the enzyme peroxidase (EC 1.11.1.7). The electron donor used in reaction (1) may be one of a number of small organic molecules or reduced nicotinamide adenine dinucleotide (NADH).[6,7]

The oscillating PO reaction is one of a few prototype (bio)chemical reaction systems, where complex dynamic behaviors have been studied extensively, both experimentally and theoretically.[8–11] The reaction has exhibited a rich variety of dynamical behaviors depending on the experimental conditions.[5,12–20]

The complex dynamics of the PO reaction has been simulated by various mathematical models. Attempts to reproduce the experimentally observed dynamics have been made using both simple hypothetical models[15,21] and more elaborated models.[22–27] One of the latter types of models is the Bronnikova–Fedkina–Schaffer–Olsen (BFSO) model,[27] listed in Table I. Numerical simulations of this model revealed the existence of extended domains of stable complex and chaotic dynamics, which are both rich and intricate.[20,28–34] The BFSO model has been successful in simulating many of the experimentally obtained dynamic behaviors, including the period-adding and period-doubling bifurcations scenarios.[17,28] However, the model has been less successful when it comes to reproducing some early experimentally observed bifurcation scenarios involving bursting oscillations.[14,15,21]

TABLE I. List of reactions and rate expressions for the BFSO model. Per(X) refers to the oxidation state of peroxidase: Per(II), ferrous peroxidase; Per(III), ferric peroxidase; Per(IV), compound II; Per(V), compound I; Per(VI), compound III. $NAD^\bullet$ is the free radical derived from one-electron oxidation of NADH. O_2^- is superoxide radical.

	Reaction	Rate expression[a]
(1)	$NADH + H^+ + O_2 \rightarrow NAD^+ + H_2O_2$	$k_1[NADH][O_2]$
(2)	$H_2O_2 + Per(III) \rightarrow H_2O + Per(V)$	$k_2[H_2O_2][Per(III)]$
(3)	$Per(V) + NADH \rightarrow Per(IV) + NAD^\bullet$	$k_3[Per(V)][NADH]$
(4)	$Per(IV) + NADH \rightarrow Per(III) + NAD^\bullet + H_2O$	$k_4[Per(IV)][NADH]$
(5)	$NAD^\bullet + O_2 \rightarrow NAD^+ + O_2^-$	$k_5[NAD^\bullet][O_2]$
(6)	$O_2^- + Per(III) \rightarrow Per(VI)$	$k_6[O_2^-][Per(III)]$
(7)	$2O_2^- + 2H^+ \rightarrow O_2 + H_2O_2$	$k_7[O_2^-]^2$
(8)	$Per(VI) + NAD^\bullet \rightarrow Per(V) + NAD^+$	$k_8[Per(VI)][NAD^\bullet]$
(9)	$2NAD^\bullet \rightarrow NAD_2$	$k_9[NAD^\bullet]^2$
(10)	$Per(III) + NAD^\bullet \rightarrow Per(II) + NAD^+$	$k_{10}[Per(III)][NAD^\bullet]$
(11)	$Per(II) + O_2 \rightarrow Per(VI)$	$k_{11}[Per(II)][O_2]$
(12)	$\rightarrow NADH$	k_{12}
(13)	$O_2(gas) \rightleftarrows O_2(liquid)$	$k_{13}([O_2]_{eq} - [O_2])$

[a]The activity of H^+ is absorbed into the rate constant.

To better understand the complex dynamical behaviors supported by the BFSO model, it would be convenient to study simplifications of the model, preferentially involving fewer variables. In the full BFSO model, the various feedback loops responsible for the origin of oscillations and complex dynamics are not obvious as is the case for the simple abstract models of the reaction.[15,21,35] Hence, it is not easy to get a detailed understanding of the individual sub-mechanisms responsible for the various kinds of complex behavior exhibited by the model. One example is the surprising and unpredictable complex behavior induced by changes in the enzyme concentration.[36] In 2006, Sensse *et al.*[37] succeeded in reducing the BFSO model to a six-variable model and, subsequently, to three simpler four-variable subnetwork models, which could be studied individually. The three four-variable subnetworks so obtained have strong similarities to three-variable extended activator–inhibitor networks introduced earlier.[38] It was possible to find conditions for homoclinic orbits and Shilnikov chaos in these simple three-variable models and in the three four-variable subnetwork models of the PO reaction.[37,38]

In the present paper, we investigate these three four-variable models further. Our investigations involve computations of isospike diagrams, namely, stability diagrams based on counting the number of spikes per period for all periodic oscillations[39,40] of the individual variables. Such diagrams are then compared with similar diagrams of the original BFSO model.[29,36] The isospike stability diagrams of the tree subnetwork models reveal complex periodic structures that enlighten and explain previous experimental observations in the PO reaction, that is, bifurcations and return maps. Two of the subnetworks also predict the existence of the recently reported quint points,[10,41–43] that is, singular points where five distinct stability phases coalesce. Finally, we present new experimental results providing evidence of quint points in the laboratory system.

II. EXPERIMENTAL SECTION

Experiments were performed in a $20 \times 20 \times 43.5$ mm quartz cuvette equipped with an oxygen electrode (Microelectrodes Inc., Bedford, NH). A stirring motor was mounted on top of the cuvette and with a stirring shaft that ended in a stirring cross 2 mm above the bottom of the cuvette. The cuvette was mounted in a Zeiss Specord S10 diode array spectrophotometer and only the spectrophotometer's tungsten lamp was used as a light source in order to avoid photochemical reactions induced by UV irradiation. The absorbencies of NADH and oxyferrous peroxidase (compound III) were recorded at 360 and 418 nm, respectively, at 2 s intervals.

The reactor had a liquid volume of 8 mL as well as an approximately 9 mL gas phase above the reaction mixture. The reaction mixture contained $0.1\,\mu M$ methylene blue, $600\,\mu M$ 4-hydroxybenzoic acid, and $2.4\,\mu M$ horseradish peroxidase, in 0.1M sodium phosphate buffer, pH 5.7 or 6.1. NADH was delivered to the reaction vessel by pumping a 0.1 M aqueous solution at a constant flow rate through a capillary tube connected to a syringe pump. The volume of the added NADH solution was negligible and balanced by an equal volume of water evaporated. Thus, the liquid volume was effectively constant at 8 mL throughout an experiment. Oxygen was supplied at atmospheric pressure to the reaction mixture via a gas mixer. The moisturized O_2/N_2 stream contained 1.05% (v/v) oxygen. The rate

of oxygen diffusion ν_{O_2} into the liquid is given by

$$\nu_{O_2} = K\left([O_2]_{eq} - [O_2]\right),$$

where $[O_2]$ is the oxygen concentration in solution, $[O_2]_{eq}$ is the oxygen concentration at equilibrium, and K is the oxygen transfer constant (equivalent to k_{13} in Table I). For a stirring rate of 1200 rpm, K was determined as $5.6 \times 10^{-3} \pm 0.1 \times 10^{-3}\,\mathrm{s}^{-1}$. Prior to the start of each experiment, the reaction mixture containing enzyme, methylene blue, and 4-hydroxybenzoic acid in buffer was thermostated at $28.0 \pm 0.1\,^{\circ}$C and equilibrated with pure nitrogen. Experiments were typically started by adding NADH at a flow rate of $50\,\mu\mathrm{L\,h}^{-1}$. As the absorbance at 360 nm reached a level close to the NADH concentration associated with a given dynamic state, the composition of the gas stream was switched from pure N_2 to the O_2/N_2 mixture. Then, the NADH flow rate was adjusted ($35-50\,\mu\mathrm{L\,h}^{-1}$) such that the NADH concentration oscillated around a constant mean level corresponding to this particular dynamic state. The dynamics were then recorded over a period of time. Thereafter, the pumping rate was changed to allow the NADH concentration to settle on another mean level associated with a different kind of behavior. Thus, changing the mean NADH concentration allows for the observation of different dynamical states as well as an unambiguous determination of the order in which they occur. Accordingly, we use the mean NADH concentration as a bifurcation parameter. This concentration was calculated using the Lambert–Beer law and an extinction coefficient of $4.3 \times 10^3\,\mathrm{M}^{-1}\,\mathrm{cm}^{-1}$ for NADH at 360 nm.[44] One could also use the NADH flow rate which, of course, determines the average NADH concentration, even though the relation between the two is nonlinear. However, this approach, while it makes for a somewhat more straightforward comparison of the data and the simulations, is less reliable. This is so because, in spite of great precautions to prepare identical NADH stock solutions, small day-to-day variations in NADH concentrations are unavoidable. If uncontrolled, these variations will necessarily affect the dynamics and are consequently a potential source of error. In short, the use of mean NADH concentration as described here removes an otherwise inevitable source of variability between experiments.

Horseradish peroxidase (RZ 3.0) and NADH disodium salt were purchased from Roche Mannheim; methylene blue was purchased from Merck. 4-Hydroxybenzoic acid was kindly provided by the Institute of Physics, Chemistry and Pharmacy, University of Southern Denmark.

III. EXTENDED ACTIVATOR–INHIBITOR MODELS OF THE PO REACTION

Oscillations and complex dynamics in the simple abstract models of the PO reaction have been studied in some detail[15,21,35] and the mechanisms responsible for the oscillations and complex dynamics are fairly well-understood. By contrast, the underlying mechanisms responsible for oscillations and complex dynamics in the detailed models are less easy to comprehend, mainly because these models may involve up to ten independent variables.[24–27] Therefore, it would be helpful if the number of variables of the more complex models could be reduced. Sensse et al.[37] managed to reduce the ten-variable BFSO scheme to a six-variable model by eliminating four redundant variables, Per(IV), Per(V), NADH, and H_2O_2 and, from

this six-variable model, they extracted three four-variable subnetwork models, which were classified as extended activator–inhibitor models.[38] Activator–inhibitor models are, in their simplest form, two-variable oscillators involving a positive and a negative feedback loop. Such models may display simple periodic oscillations. But when extended with a third variable and an additional feedback loop, they may exhibit complex periodic oscillations and homoclinic behavior (chaos).[38]

The three subnetwork models derived from the reduced six-variable BFSO model share a common reaction core constituted by reactions (1)–(8) in Table II. The reaction numbers refer to the numbers in the original publication.[37] These reactions – involving the species $NAD^\bullet$, O_2, and Per(VI)—form a minimal reaction core for oscillatory behavior. This minimal core displays purely periodic oscillations. In order to allow for complex dynamics and chaos, the core reactions (1)–(8) must be extended with an additional feedback from an additional variable, which may be either O_2^-, Per(II) or Per(III) as described by reaction (13), reactions (11)–(12), or reactions (9)–(10) in Table II, respectively.[37] The core reactions (1)–(8) and the supplementary reactions listed in Table II form the three subnetwork models. It is worth pointing out that the reactions of the subnetworks do not always make an obvious chemical sense as they have been constructed by lumping together reactions from Table I. In this lumping process, some reactants and products that do not enter into the resulting differential equations have been omitted. For example, reaction (1) in Table II is the result of lumping reactions (8), (3), and (4) in Table I. Furthermore, since NADH is not a variable in these reduced models, there is also no inflow

TABLE II. List of reactions and rate expressions for the three subnetwork models (subnetworks 1, 2, and 3) of the PO reaction. Each subnetwork consists of the core reactions (1)–(8) plus either reaction (13) (subnetwork 1), reactions (11)–(12) (subnetwork 2), or reactions (9)–(10) (subnetwork 3). The meanings of Per(II), Per(III), and Per(VI) are the same as in Table I.

	Reaction	Rate expression
	Core reactions	
(1)	$NAD^\bullet + Per(VI) \rightarrow 2NAD^\bullet + Per(III)$	$k_1[NAD^\bullet][Per(VI)]$
(2)	$NAD^\bullet + O_2 \rightarrow NAD^+ + O_2^-$	$k_2[NAD^\bullet][O_2]$
(3)	$2NAD^\bullet \rightarrow (NAD)_2$	$k_3[NAD^\bullet]^2$
(4)	$\rightarrow NAD^\bullet$	k_4
(5)	$O_2 \rightarrow$	$k_5[O_2]$
(6)	$\rightarrow O_2$	k_6
(7)	$Per(VI) \rightarrow$	$k_7[Per(VI)]$
(8)	$\rightarrow Per(VI)$	k_8
	Subnetwork 1	
(13)	$2O_2^- + 2H^+ \rightarrow O_2$	$k_{13}[O_2^-]^2$
	Subnetwork 2	
(11)	$NAD^\bullet + Per(III) \rightarrow Per(II)$	$k_{11}[NAD^\bullet]$
(12)	$O_2 + Per(II) \rightarrow Per(VI)$	$k_{12}[O_2][Per(II)]$
	Subnetwork 3	
(9)	$Per(III) \rightarrow Per(VI)$	$k_9[Per(III)]$
(10)	$Per(III) \rightarrow$	$k_{10}[Per(III)]$

of this [reaction (12) in Table I]. This role is, according to Sensse *et al.*,[37] instead played by reaction (4) in Table II. Also, enzyme intermediates are created and destroyed in an unbalanced way, e.g., in reactions (7), (8), and (10) in Table II. This precludes the conservation of total enzyme concentration. In the BFSO model (and in the experimental system), the sum of all concentrations of enzyme forms (namely, [Per(II)]+[Per(III)]+[Per(IV)]+[Per(V)]+[Per(VI)]) is a constant and hence the total concentration of an enzyme can be used as a parameter.[36]

Sensse *et al.* have shown[37] that homoclinic orbits and Shilnikov chaos occur in all three subnetworks as well as in the reduced six-variable BFSO model. This suggests that Shilnikov chaos may be also present in the original ten-variable BFSO model and, therefore, also in the experimental system. Previously, circumstantial evidence for homoclinic chaos has been presented, both in the experimental PO reaction[20] and in the BFSO model, but this evidence was based on the similarity of return maps to those of a standard equation exhibiting homoclinic chaos and hence is only indirect.

The ODEs of the three subnetwork models listed below were simulated and isospike stability diagrams were computed as described in detail previously.[36] We used the standard fourth-order Runge–Kutta integrator with fixed step-size $h = 0.01$, *following the attractor* horizontally from right to left, from the initial conditions given below. The steady states, eigenvalues, Jacobian matrices, Lyapunov exponents (to estimate Kaplan–Yorke dimension[45]), and return maps obtained from Poincaré sections were computed using the COPASI software.[46] The computations of eigenvalues confirmed that the steady states corresponding to chaotic behavior were saddle foci with a complex pair of eigenvalues and two real eigenvalues. The real part of the complex pair was positive, while the real eigenvalues were negative.

A. Subnetwork 1

This subnetwork model is, like the other two subnetwork models, centered around a basic core mechanism, which includes reactions (1)–(8) in Table II. These reactions form a three-variable mechanism, which involves an autocatalytic reaction [reaction (1)] and a negative feedback [reaction (3)], and allow for only simple periodic oscillations. However, extending this mechanism with O_2^- as a fourth variable [through reactions (2) and (13)] creates an extra positive feedback loop between O_2 and O_2^- as can be seen from
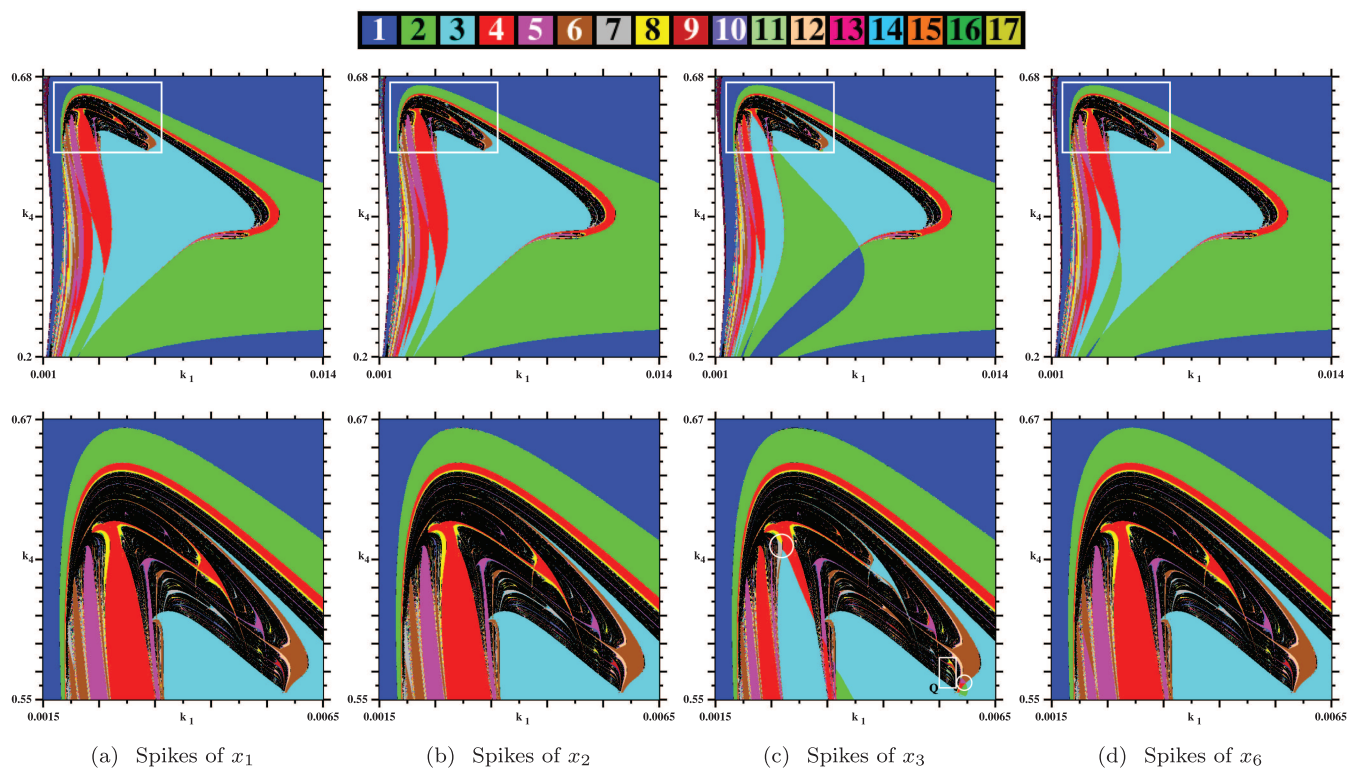
FIG. 1. Stability diagrams for subnetwork 1, obtained by counting spikes for the four variables in Eqs. (2)–(5), and plotting them recycling colors modulo 17. Top row: global view. Bottom row: magnifications of the white boxes seen on the top row. Quint points are located at the center of the white circles in the diagram for variable x_3. The rectangle near Q is magnified in Fig. 2 and illustrates many additional quint points. The distribution of spikes recorded for x_3 contains several additional features not present in the distributions recorded for the other three variables.

the Jacobian matrix.[37] This makes it possible for the model to show complex dynamical behavior. Using the rate expressions in Table II, one obtains[37] the following ODEs for subnetwork 1:

$$\frac{dx_1}{dt} = k_1 x_1 x_3 - k_2 x_1 x_2 - 2k_3 x_1^2 + k_4, \tag{2}$$

$$\frac{dx_2}{dt} = -k_2 x_1 x_2 - k_5 x_2 + k_6 + k_{13} x_6^2, \tag{3}$$

$$\frac{dx_3}{dt} = -k_1 x_1 x_3 - k_7 x_3 + k_8, \tag{4}$$

$$\frac{dx_6}{dt} = k_2 x_1 x_2 - 2k_{13} x_6^2. \tag{5}$$

Here, x_1, x_2, x_3, and x_6 represent NAD$^\bullet$, O$_2$, Per(VI) (compound III), and O$_2^-$, respectively. The rate constants are $k_2 = 0.415$, $k_3 = 0.007$, $k_5 = 0.14$, $k_6 = 0.71$, $k_7 = 10^{-4}$, $k_8 = 0.353$, $k_{13} = 6 \times 10^{-4}$, while k_1 and k_4 vary in the intervals defined in Fig. 1. Suitable initial conditions are $x_1(0) = 1$, $x_2(0) = 2$, $x_3(0) = 20$, and $x_6(0) = 20$.

B. Subnetwork 2

Subnetwork 2, like subnetwork 1, involves NAD$^\bullet$, O$_2$, and Per(VI) in the core mechanism. However, in this model, the fourth variable is Per(II), which participates in reactions (11) and (12) in Table II. This creates an additional positive feedback between NAD$^\bullet$, Per(VI), and Per(II).[37] The equations that can be derived from the rate expressions in Table II are

$$\frac{dx_1}{dt} = k_1 x_1 x_3 - k_2 x_1 x_2 - 2k_3 x_1^2 + k_4 - k_{11} x_1, \tag{6}$$

$$\frac{dx_2}{dt} = -k_2 x_1 x_2 - k_5 x_2 + k_6 - k_{12} x_2 x_5, \tag{7}$$

$$\frac{dx_3}{dt} = -k_1 x_1 x_3 - k_7 x_3 + k_8 + k_{12} x_2 x_5, \tag{8}$$

$$\frac{dx_5}{dt} = k_{11} x_1 - k_{12} x_2 x_5. \tag{9}$$

Here, x_1, x_2, x_3, and x_5 represent NAD$^\bullet$, O$_2$, Per(VI), and Per(II), respectively. The rate constants are $k_2 = 0.15$, $k_3 = 0.008$, $k_5 = 0.132$, $k_6 = 1$, $k_7 = 0.01$, $k_8 = 0.59$, $k_{11} = 0.23$, $k_{12} = 0.015$, and k_1 and k_4 as defined in Fig. 3. Initial conditions are $x_1(0) = 1$, $x_2(0) = 2$, $x_3(0) = 20$, and $x_5(0) = 20$.

C. Subnetwork 3

Subnetwork 3 has Per(III) as its fourth variable through reactions (9) and (10) in Table II. From the Jacobian matrix, it can be inferred that it has a positive feedback loop between NAD$^\bullet$, Per(VI), and Per(III) and an additional positive feedback loop between Per(VI) and Per(III). The equations that can be derived from the
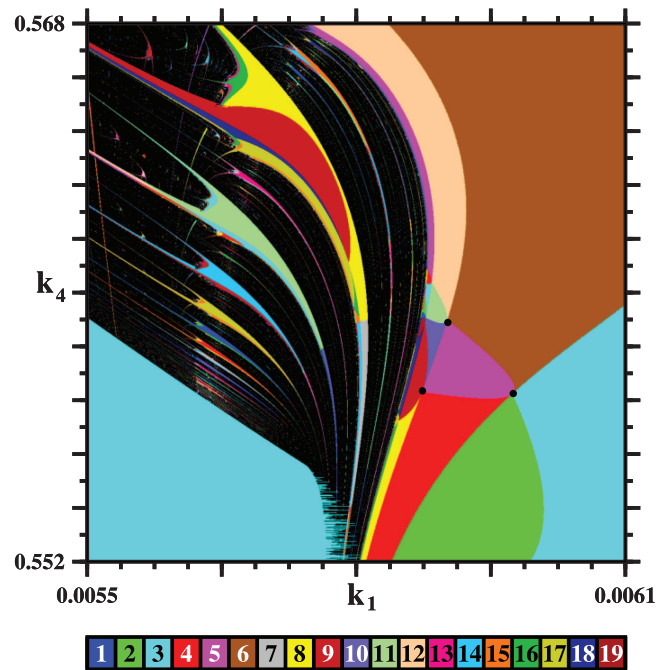

FIG. 2. Magnification of the rectangle near Q in Fig. 1. The distribution of spikes recorded for x_3 contains several additional features not present in the distributions recorded for the other three variables. The three black dots indicate the location of *quint points*, the first of a discrete network of points where five oscillatory modes with a distinct number of spikes per period coalesce. Color coding has the same meaning as in Fig. 1.

rate expressions in Table II are

$$\frac{dx_1}{dt} = k_1 x_1 x_3 - k_2 x_1 x_2 - 2k_3 x_1^2 + k_4, \tag{10}$$

$$\frac{dx_2}{dt} = -k_2 x_1 x_2 - k_5 x_2 + k_6, \tag{11}$$

$$\frac{dx_3}{dt} = -k_1 x_1 x_3 - k_7 x_3 + k_8 + k_9 x_4, \tag{12}$$

$$\frac{dx_4}{dt} = k_1 x_1 x_3 - k_9 x_4 - k_{10} x_4. \tag{13}$$

Here, x_1, x_2, x_3, and x_4 represent NAD$^\bullet$, O$_2$, Per(VI), and Per(III), respectively. The rate constants are $k_2 = 0.3$, $k_3 = 0.008$, $k_5 = 0.285$, $k_6 = 1.25$, $k_7 = 10^{-3}$, $k_8 = 0.07$, $k_9 = 0.052$, $k_{10} = 0.003\,96$, and k_1 and k_4 as shown in Fig. 4. Initial conditions are $x_1(0) = 1$, $x_2(0) = 2$, $x_3(0) = 20$, and $x_4(0) = 20$.

IV. STABILITY DIAGRAMS AND BIFURCATION SCENARIOS OF SUBNETWORKS 1, 2, AND 3

One goal of the current study is to compare transitions between different states of complex behaviors in the three subnetwork models to those of the corresponding transitions observed

in the original BFSO model[29,36] and in experiments of the PO reaction.[14,17,20] Most of these experiments were conducted at enzyme concentrations between 0.5×10^{-6} and 1.5×10^{-6}M. In our recent study of complex dynamics in the BFSO model at different concentrations of peroxidase,[36] we showed that at enzyme concentrations below 2×10^{-6}M, the dynamics is dominated by subnetworks 1 and 3, while subnetwork 2 seems to play a minor role. As the enzyme concentration is increased, the contribution of subnetwork 2 increases from close to zero and becomes dominant at enzyme concentrations around 5×10^{-6}M or more.[36]

In several experimental studies, the flow rate of NADH is used as a bifurcation parameter.[20,28] Therefore, one of the parameters to vary is rate constant k_4, which, as mentioned in the previous section, was suggested to represent the inflow of NADH.[37] As the second parameter in the isospike stability diagrams, we have chosen rate constant k_1, which determines the rate of the autocatalytic reaction.

Figure 1 shows isospike stability diagrams for subnetwork 1, Eqs. (2)–(5), while isospike diagrams of subnetworks 2 and 3 are shown in Figs. 3 and 4, respectively. None of these diagrams are structurally similar to the ones obtained for the original BFSO model,[29,36] although there is some resemblance of the diagram obtained for subnetwork 1 to a diagram obtained for the original BFSO model at an enzyme concentration of 1.8×10^{-6} M.[36] For example, in the experimental system and in the original BFSO

model, the dynamics begins with simple periodic oscillations at low flow rates of NADH and becomes more complex as this flow rate increases. However, while, according to Sensse et al.,[37] k_4 represents the NADH flow rate in the reduced six-variable model and in the three four-variable subnetworks, such a transition from simple periodic oscillations to still more complex oscillations as k_4 is increased is only observed in the subnetwork 1 diagram. In the subnetwork 2 diagram, the transition from simple periodic oscillations to complex dynamics happens when k_4 is decreased and in the subnetwork 3 diagram, neither period-doubling nor period-adding bifurcations can be observed when k_4 is changed.

The black regions in the diagrams in Figs. 1–4 represent non-periodic dynamics, which again represent chaotic dynamics. Magnifications of these black (chaotic) domains reveal many shrimp-shaped isospike domains.[47,48] Unlike the BFSO model, where some non-periodic domains represent quasiperiodic dynamics,[30,31,49] we have not yet found evidence for quasiperiodic oscillations in the three subnetwork models studied here.

In spite of the different forms of the isospike diagrams of the three subnetworks compared to the diagrams of the original BFSO scheme, there are some interesting and relevant results obtained from the isospike diagrams in Figs. 1–4. For example, increasing the rate constant k_1 for the three subnetworks is analogous to increasing the concentration of the aromatic cofactors

(a) Spikes of x_1 (b) Spikes of x_2 (c) Spikes of x_3 (d) Spikes of x_5
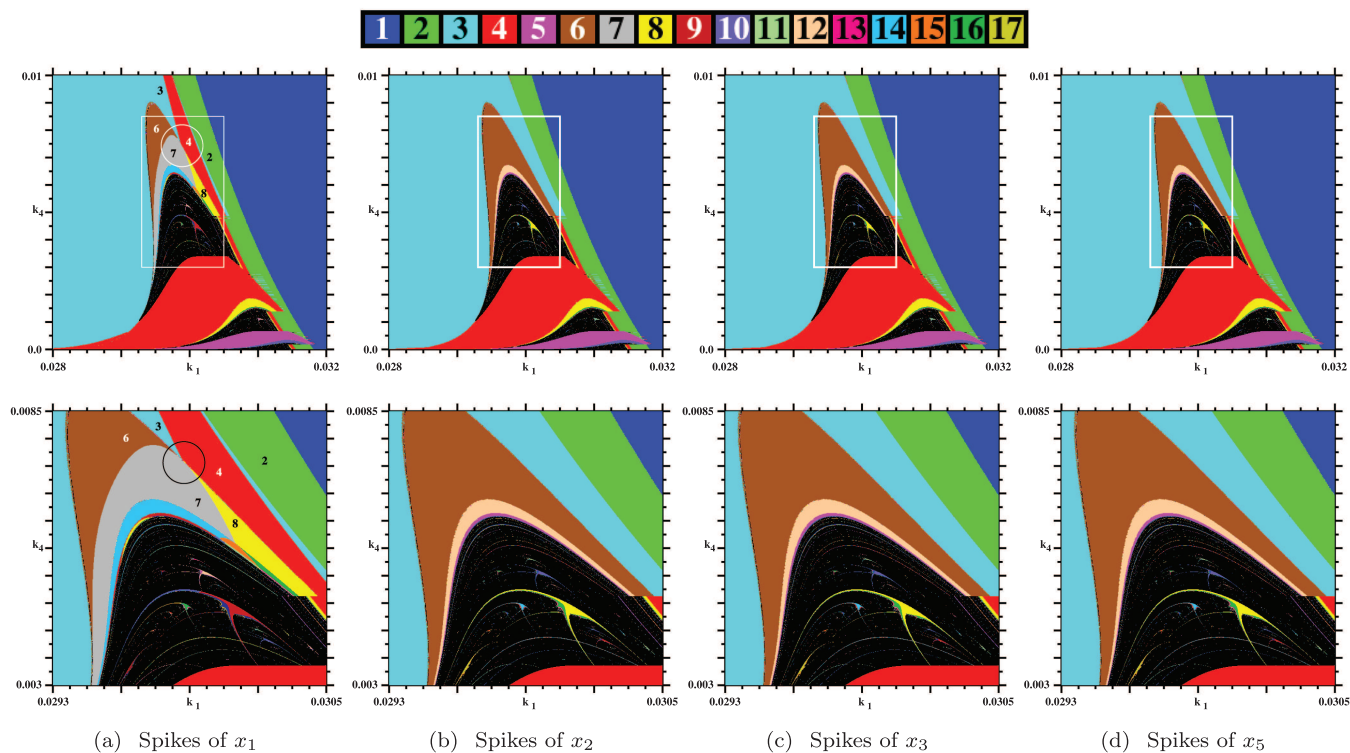
FIG. 3. Stability diagrams for subnetwork 2, obtained by counting spikes for the four variables in Eqs. (6)–(9), and plotting them recycling colors modulo 17. Top row: global view. Bottom row: magnifications of the white boxes seen on the top row. A quint point is located at the center of the circles in the diagram for variable x_1. The distribution of spikes recorded for x_1 is markedly distinct from the distributions for the other three variables.
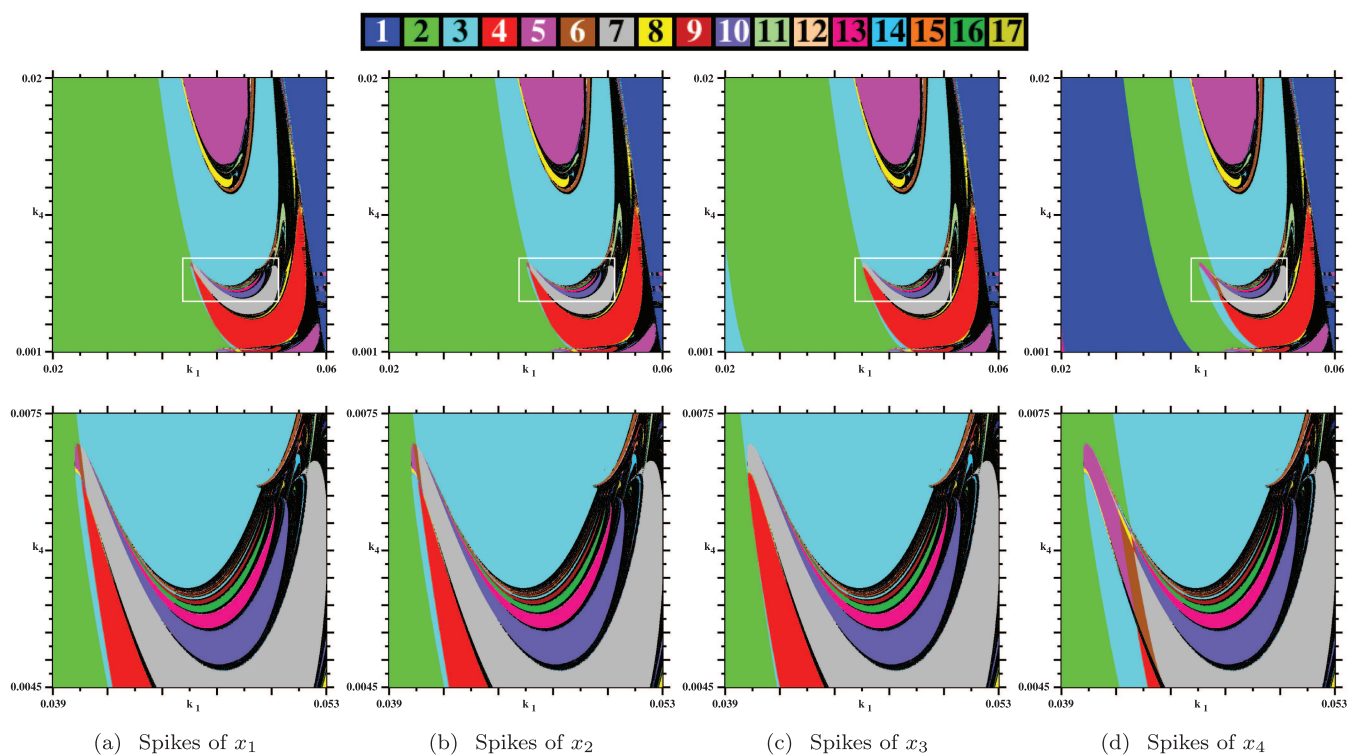
FIG. 4. Stability diagrams for subnetwork 3, obtained by counting spikes for the four variables in Eqs. (10)–(13), and plotting them recycling colors modulo 17. Top row: global view. Bottom row: magnifications of the white boxes seen on the top row.

such as 2,4-dichlorophenol.[15] It was previously shown that a period-doubling route to chaos could be observed when the concentration of 2,4-dichlorophenol was increased.[17] The same is the case if we increase the rate constant k_1 in the subnetwork 1 model (from around 0.0015 to 0.003). Likewise, it may be argued that the rate of reaction 1 will also increase if the concentration of peroxidase increases. Previously, it was shown experimentally that a decrease in the concentration of peroxidase may induce a transition from simple periodic oscillations to chaos to bursting oscillations.[14,15] Here, a similar observation can be made for subnetwork 3 following a decrease in the rate constant k_1 (from 0.06 to around 0.045). However, the bursting oscillations obtained here are slightly different from those observed in the experiments.[14,15] Also, the leftmost spike distributions recorded for x_1, x_2, and x_4 in Fig. 4 show regions with *spikes mosaics* observed earlier in chaos-free regions.[50]

Another interesting result is the observation of quint points in subnetworks 1 and 2 (see Figs. 1 and 3).[10,41,42] A quint point is a point where five distinct isospike phases meet. An example of such a point can be observed in the upper left panel of Fig. 3 (variable x_1). In this case, the five phases are oscillations with 3, 4, 6, 7, and 8 spikes per period. Further magnifications (not shown here) reveal additional quint points, but these are rather compressed. Similar quint points can be spotted in the lower panel of Fig. 1 (variable x_3). A magnification of the white rectangle next to the Q in Fig. 1(c) (shown in Fig. 2)

reveals three quint points, and further magnifications of this region (not shown) show cascades of additional quint points. Interestingly, new experiments have now revealed evidence for such quint points.

Figure 5 shows the time series of the absorbance at 418 nm due to Per(VI) (compound III) at two different pH values (pH 5.7 and pH 6.1) and at different mean concentrations of NADH, corresponding to different flow rates of NADH. In Fig. 5(a) (pH 5.7), the dynamics change from oscillations with two spikes per period to oscillations with four spikes per period to oscillations with eight spikes per period as the mean NADH concentration is increased. In Fig. 5(b), the corresponding transitions are from three spikes per period to six spikes per period, to seven spikes per period. In the diagram in Fig. 5(c), we show an experimental isospike diagram with all complex periodic and non-periodic states plotted against the mean NADH level. We note that at a mean NADH concentration from about 134 μM to about 142 μM, we observe a similar pattern of periodic states as in the left panel of Fig. 3 when k_4 is decreased. It is noteworthy that these experiments are performed with a peroxidase concentration of 2.4 μM, i.e., higher than in previously reported experiments[20,28,36] and in the concentration range where subnetwork 2 is supposed to play a more significant role.[36] It is worth pointing out that so far quint points have not yet been reported for the original BFSO model although it seems reasonable to conjecture their existence.
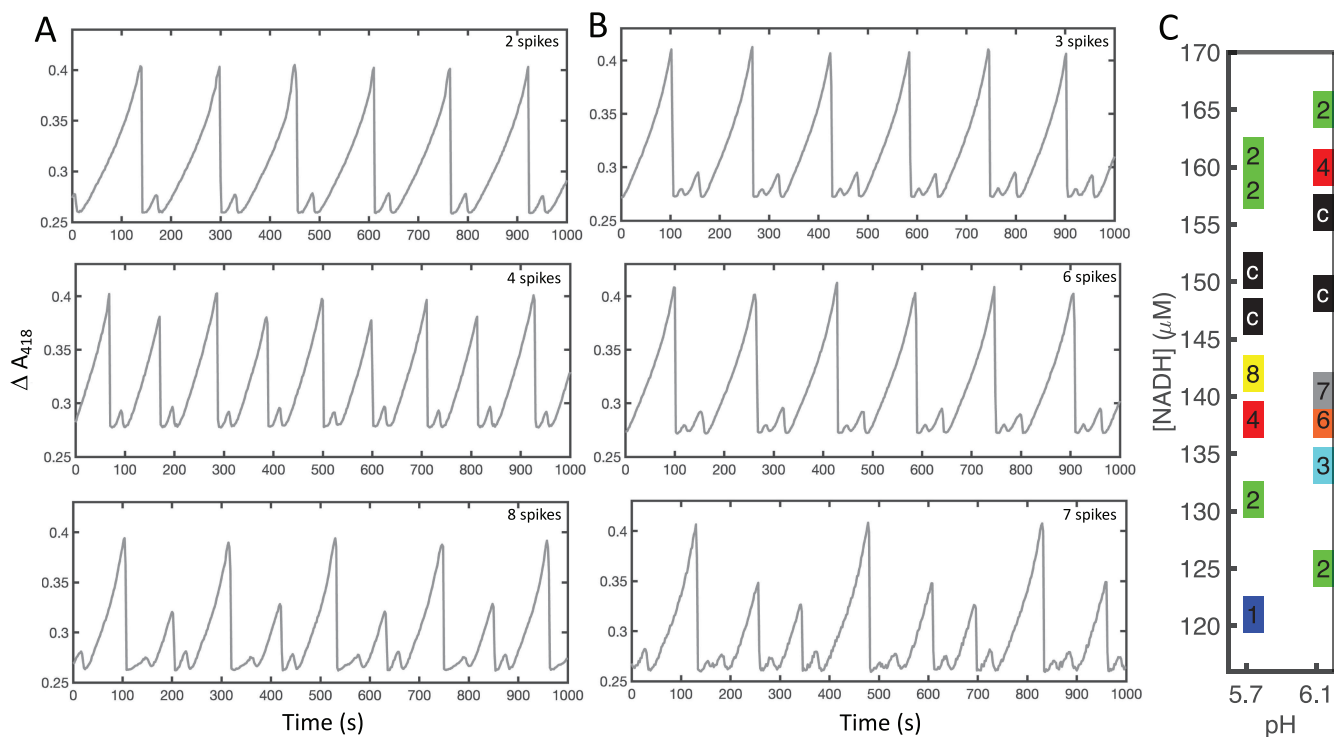
FIG. 5. Evidence for a quint point in the experimental PO reaction. (a) and (b) are plots of the absorbance at 418 nm against time. The time series in (a) were recorded at pH 5.7, while the series in (b) were recorded at pH 6.1. In (c), we show the number of spikes per period plotted as a function of the mean NADH concentration at which the oscillations were obtained. (c) indicates non-periodic (chaotic) oscillations. The experiments were conducted in 0.1M phosphate buffer, pH 5.7 or 6.1. The reaction mixture contained 2.4 μM horseradish peroxidase, 600 μM 4-hydroxybenzoic acid, and 0.1 μM methylene blue. Each experiment was started with an initial concentration of NADH of 0 μM and an oxygen concentration of 0 μM. NADH was pumped into the reaction mixture until it reached a concentration between 120 and 170 μM. Then, the oxygen in the gas stream was switched from 0% to 1.05% (v/v) and the pumping rate was adjusted such that the NADH concentration settled on a constant mean level, and the dynamics of Per(VI) (absorbance at 418 nm) was recorded for at least 1000 s. Other experimental conditions as stated in Sec. II.
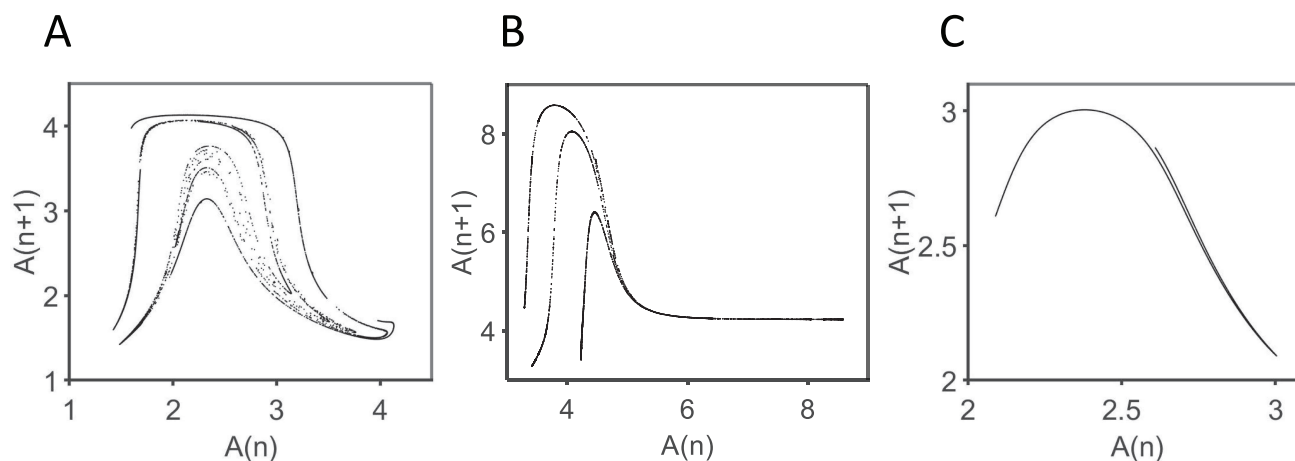
FIG. 6. Return maps (next-amplitude maps) of O_2 (x_2) obtained for representative chaotic oscillations of (a) subnetwork 3 when $k_1 = 0.0546$ and $k_4 = 0.0077$, (b) subnetwork 2 when $k_1 = 0.031$ and $k_4 = 0.0008$, and (c) subnetwork 1 when $k_1 = 0.0065$ and $k_4 = 0.58$.

We also computed return maps for chaotic oscillations for all three subnetworks. These are shown in Fig. 6. We note that the map for subnetwork 3 shown in Fig. 6(a) resembles the experimental map found in early experimental data from the PO reaction[14,21] while the map for subnetwork 1 shown in Fig. 6(c) resembles subsequent experimental maps.[17,20] The map obtained for subnetwork 2 shown in Fig. 6(b) appears somewhat "in between" the maps for the other two subnetworks. Such a map has not yet been observed in the experimental system. The transition from fractal to almost 1D return map as we go from Figs. 6(a) to 6(c) is supported by computations of Kaplan–Yorke D_{KY} dimension.[45] The attractor corresponding to the return map in 6(a) has a $D_{KY} = 2.13$, while the attractors corresponding to return maps in Figs. 6(b) and 6(c) have D_{KY} of 2.11 and 2.08, respectively. For comparison, a very recent computation[51] for the Lorenz attractor reports $D_{KY} = 2.06$.

V. DISCUSSION

In the present paper, we have studied three four-variable subnetwork models derived from the ten-variable BFSO model of the PO reaction.[37] The three subnetworks belong to the class of extended activator–inhibitor systems.[37,38] Our study involved the construction of isospike stability diagrams to get an overview of the possible complex dynamics states for these subnetworks and their mutual placement in control parameter space. We also tested the complexity states of the subnetworks against states of complexity observed in the original BFSO model and in the experimental system. It is interesting that the three subnetworks reproduce distinct aspects obtained in the experimental system under different experimental conditions. Subnetwork 1 is capable of reproducing the experimental observation of a period-doubling cascade when the concentration of the phenolic modifier (e.g., 2,4-dichlorophenol) is increased and the corresponding almost 1D return map of chaotic fluctuations of oxygen concentration.[17] It is also capable of reproducing the observation of both period-doubling and period-adding cascades[20,28] when the flow rate of NADH is increased. Subnetwork 3 is capable of reproducing the experimental observation of chaotic fluctuations situated between simple periodic oscillations and bursting oscillations and the corresponding fractal-like return maps.[14,15,21] Thus, it appears that subnetwork 3 has some resemblance to another simple four-variable model of the PO reaction.[21]

As for the structures of the isospike stability diagrams, they appear distorted compared to those of the original BFSO model.[36] In a previous study[36] of the original BFSO model we have shown that the isospike stability diagrams undergo a "crystallization" process as the initial concentration of Per(III) is increased. It is interesting to note that one of these diagrams has some resemblance to the diagram of subnetwork 1 studied here. Unfortunately, there is no preservation of enzyme in any of the three subnetwork models, so the total concentration of the enzyme cannot serve as a parameter for them. Hence, a similar "crystallization" of isospike diagrams, when the enzyme concentration is increased, cannot be explored for the three subnetwork models. An interesting discrepancy between the isospike diagrams for the three subnetworks and those of the original BFSO model involves the rate constant k_4, which determines the constant influx of NAD$^\bullet$ and, according to

Sensse et al.,[37] may be considered equivalent to the influx of NADH (determined by the rate constant k_{12} in Table I). This claim only seems to hold for subnetwork 1, where an increase of k_4 results in transitions from simple periodic oscillations to still more complex oscillations and chaos through either period-doubling or period-adding bifurcations as is also the case for the original BFSO model when k_{12} is increased (at least for an enzyme concentration lower than 2×10^{-6}M).[36]

It should also be mentioned that the subnetworks studied here deviate from the original BFSO model in that contrary to the original BFSO model, where quasiperiodic oscillations can be observed for certain parameters,[30,33,49] analogous quasiperiodic behavior has yet to be detected in the three subnetwork models. The latter is also at variance with the experimental PO reaction in which various forms of quasiperiodicity can be found.[18,19,30,33,49] It is likely that quasiperiodicity is lost or strongly reduced by the simplification of the original BFSO model.

Finally, we have found that subnetworks 1 and 2 both reveal the existence of quint points, i.e., very recently reported singular boundary points where five distinct phases of stable oscillatory behavior meet in isospike diagrams.[10,41–43] Evidence for such a quint point could also be found in recent experimental data at elevated concentrations of peroxidase. Thus, overall the three subnetworks display complex behavior in good correspondence with previous and our present experimental data. Some of these, e.g. the occurrence of quint points and the fractal return maps shown in Fig. 6(a), have yet to be found in the original BFSO model.

We conclude that the isospike stability diagrams have proved extremely valuable in analyzing and understanding the complex dynamics of the subnetworks, the original BFSO model, as well as the experimental PO reaction. Subnetwork 1 has the closest resemblance to the original BFSO model both in terms of the bifurcation structure and the structure of return maps. The other two subnetworks are structurally different but also reproduce important observations in the experimental system such as fractal return maps (subnetwork 3) and the appearance of quint points (subnetwork 2). Thus, the three subnetwork models may be taken as well representing significant aspects of the PO reaction. In particular, the fact that two subnetworks display quint points, which were also detected experimentally, exposes an intriguing open problem: to investigate the possibility of detecting the recently reported phenomenon of *non-quantum chirality*[40,43] among the rich realm of complex behaviors displayed by the PO reaction, its subnetwork models, and similar (bio)chemical complex systems. Non-quantum chirality refers to surprising chiral structures observed recently in the nonlinear oscillators governed by rate equations, not by any quantum feature.[40–43]

AUTHOR DECLARATIONS

Conflict of Interest

The authors have no conflicts to disclose.

Author Contributions

Jason A. C. Gallas: Conceptualization (equal); Formal analysis (equal); Investigation (equal); Software (equal); Writing – original draft (equal); Writing – review & editing (equal). **Lars F. Olsen:** Conceptualization (equal); Formal analysis (equal); Writing – original draft (equal); Writing – review & editing (equal).

DATA AVAILABILITY

The data that support the findings of this study are available from the corresponding author upon reasonable request.

REFERENCES

[1] K. Poole, "A review of the Canada Lynx, Lynx canadensis, in Canada," Can. Field-Nat. **117**, 360–376 (2003).

[2] L. Glass, "Synchronization and rhythmic processes in physiology," Nature **410**, 277–284 (2001).

[3] N. M. Woods, K. S. R. Cuthbertson, and P. H. Cobbold, "Repetitive transient rises in cytoplasmic free calcium in hormone-stimulated hepatocytes," Nature **319**, 600–602 (1986).

[4] B. Hess, "Periodic patterns in biochemical reactions," Q. Rev. Biophys. **30**, 121–176 (1997).

[5] S. Nakamura, K. Yokota, and I. Yamazaki, "Sustained oscillations in a lactoperoxidase NADPH and O_2 system," Nature **222**, 794 (1969).

[6] A. Scheeline, D. L. Olson, E. P. Williksen, G. A. Horras, M. L. Klein, and R. Larter, "The peroxidase-oxidase oscillator and its constituent chemistries," Chem. Rev. **97**, 739–756 (1997).

[7] H. B. Dunford, *Heme Peroxidases* (Wiley-VCH, 1999).

[8] *Chaos in Chemistry and Biochemistry*, edited by R. J. Field and L. Györgyi (World Scientific, Singapore, 1993).

[9] R. J. Field, "Chaos in the Belousov-Zhabotinsky reaction," Mod. Phys. Lett. B **29**, 1530015 (2015).

[10] R. J. Field, J. G. Freire, and J. A. C. Gallas, "Quint points lattice in a driven Belousov-Zhabotinsky reaction model," Chaos **31**, 053124 (2021).

[11] J. Maselko and I. R. Epstein, "Chemical chaos in the chlorite-thiosulfate reaction," J. Chem. Phys. **80**, 3175–3178 (1984).

[12] I. Yamazaki, K. Yokota, and R. Nakajima, "Oscillatory oxidations of reduced pyridine nucleotide by peroxidase," Biochem. Biophys. Res. Commun. **21**, 582–586 (1965).

[13] H. Degn, "Compound-3 kinetics and chemiluminescence in oscillatory oxidation reactions catalyzed by horseradish peroxidase," Biochim. Biophys. Acta **180**, 271–290 (1969).

[14] L. F. Olsen and H. Degn, "Chaos in an enzyme reaction," Nature **267**, 177–178 (1977).

[15] L. F. Olsen and H. Degn, "Oscillatory kinetics of peroxidase-oxidase reaction in an open system–Experimental and theoretical studies," Biochim. Biophys. Acta **523**, 321–334 (1978).

[16] B. D. Aguda, L. L. H. Frisch, and L. Olsen, "Experimental-evidence for the coexistence of oscillatory and steady-states in the peroxidase-oxidase reaction," J. Am. Chem. Soc. **112**, 6652–6656 (1990).

[17] T. Geest, C. G. Steinmetz, R. Larter, and L. F. Olsen, "Period-doubling bifurcations and chaos in an enzyme reaction," J. Phys. Chem. **96**, 5678–5680 (1992).

[18] M. S. Samples, Y.-F. Hung, and J. Ross, "Further experimental studies on the horseradish-peroxidase oxidase reaction," J. Phys. Chem. **96**, 7338–7342 (1992).

[19] T. Hauck and F. W. Schneider, "Mixed-mode and quasi-periodic oscillations in the peroxidase oxidase reaction," J. Phys. Chem. **97**, 391–397 (1993).

[20] M. J. B. Hauser and L. F. Olsen, "Mixed-mode oscillations and homoclinic chaos in an enzyme reaction," J. Chem. Soc., Faraday Trans. **92**, 2857–2863 (1996).

[21] L. F. Olsen, "An enzyme reaction with a strange attractor," Phys. Lett. A **94**, 454–457 (1983).

[22] K. Yokota and I. Yamazaki, "Analysis and computer-simulation of aerobic oxidation of reduced nicotinamide adenine-dinucleotide catalyzed by horseradish-peroxidase," Biochemistry **16**, 1913–1920 (1977).

[23] V. R. Fedkina, F. I. Ataullakhanov, and T. V. Bronnikova, "Computer-simulation of sustained oscillations in peroxidase-oxidase reaction," Biophys. Chem. **19**, 259–264 (1984).

[24] B. D. Aguda and R. Larter, "Sustained oscillations and bistability in a detailed mechanism of the peroxidase oxidase reaction," J. Am. Chem. Soc. **112**, 2167–2174 (1990).

[25] B. D. Aguda and R. Larter, "Periodic chaotic sequences in a detailed mechanism of the peroxidase-oxidase reaction," J. Am. Chem. Soc. **113**, 7913–7916 (1991).

[26] D. L. Olson, E. P. Williksen, and A. Scheeline, "An experimentally based model of the peroxidase-NADH biochemical oscillator—An enzyme-mediated chemical switch," J. Am. Chem. Soc. **117**, 2–15 (1995).

[27] T. V. Bronnikova, V. R. Fed'kina, W. M. Schaffer, and L. F. Olsen, "Period-doubling bifurcations and chaos in a detailed model of the peroxidase-oxidase reaction," J. Phys. Chem. **99**, 9309–9312 (1995).

[28] M. J. B. Hauser, L. F. Olsen, T. V. Bronnikova, and W. M. Schaffer, "Routes to chaos in the peroxidase-oxidase reaction: Period-doubling and period-adding," J. Phys. Chem. B **101**, 5075–5083 (1997).

[29] M. J. B. Hauser and J. A. C. Gallas, "Nonchaos-mediated mixed-mode oscillations in an enzyme reaction system," J. Phys. Chem. Lett. **5**, 4187–4193 (2014).

[30] T. V. Bronnikova, W. M. Schaffer, and L. F. Olsen, "Quasiperiodicity in a detailed model of the peroxidase-oxidase reaction," J. Chem. Phys. **105**, 10849–10859 (1996).

[31] T. V. Bronnikova, W. M. Schaffer, M. J. B. Hauser, and L. F. Olsen, "Routes to chaos in the peroxidase-oxidase reaction. 2. The fat torus scenario," J. Phys. Chem. B **102**, 632–640 (1998).

[32] T. V. Bronnikova, W. M. Schaffer, and L. F. Olsen, "Nonlinear dynamics of the peroxidase-oxidase reaction: I. Bistability and bursting oscillations at low enzyme concentrations," J. Phys. Chem. B **105**, 310–321 (2001).

[33] L. F. Olsen, T. V. Bronnikova, and W. M. Schaffer, "Secondary quasiperiodicity in the peroxidase-oxidase reaction," Phys. Chem. Chem. Phys. **4**, 1292–1298 (2002).

[34] W. M. Schaffer, T. V. Bronnikova, and L. F. Olsen, "Nonlinear dynamics of the peroxidase-oxidase reaction. II. Compatibility of an extended model with previously reported model-data correspondences," J. Phys. Chem. B **105**, 5331–5340 (2001).

[35] H. Degn, L. F. Olsen, and J. W. Perram, "Bistability, oscillation and chaos in an enzyme reaction," Ann. N. Y. Acad. Sci. **316**, 623–637 (1979).

[36] J. A. C. Gallas, M. J. B. Hauser, and L. F. Olsen, "Complexity of a peroxidase-oxidase reaction model," Phys. Chem. Chem. Phys. **23**, 1943–1955 (2021).

[37] A. Sensse, M. J. B. Hauser, and M. Eiswirth, "Feedback loops for Shilnikov chaos: The peroxidase-oxidase reaction," J. Chem. Phys. **125**, 014901 (2006).

[38] A. Sensse and M. Eiswirth, "Feedback loops for chaos in activator-inhibitor systems," J. Chem. Phys. **122**, 044516 (2005).

[39] J. G. Freire and J. A. C. Gallas, "Stern-Brocot trees in the periodicity of mixed-mode oscillations," Phys. Chem. Chem. Phys. **13**, 12191–12198 (2011).

[40] J. A. C. Gallas, "Non-quantum chirality in a driven Brusselator," J. Phys.: Condens. Matter **34**, 144002 (2022).

[41] J. A. C. Gallas, "Chirality detected in Hartley's electronic oscillator," Eur. Phys. J. Plus **136**, 59 (2021).

[42] J. A. C. Gallas, "Chirality observed in a driven ruthenium-catalyzed Belousov–Zhabotinsky reaction model," Phys. Chem. Chem. Phys. **23**, 25720–25726 (2021).

[43] C. K. Volos and J. A. C. Gallas, "Experimental evidence of quint points and non-quantum chirality in a minimalist autonomous electronic oscillator," Eur. Phys. J. Plus **137**, 527 (2022).

[44] M. J. B. Hauser, U. Kummer, A. Z. Larsen, and L. F. Olsen, "Oscillatory dynamics protect enzymes and possibly cells against toxic substances," Faraday Discuss. **120**, 215–227 (2002).

[45]P. Frederickson, J. L. Kaplan, E. D. Yorke, and J. A. Yorke, "The Lyapunov dimension of strange attractors," J. Differ. Equ. **49**, 185–207 (1983).

[46]S. Hoops, S. Sahle, R. Gauges, C. Lee, J. Pahle, N. Simus, M. Singhal, L. Xu, P. Mendes, and U. Kummer, "Copasi—A complex pathway simulator," Bioinformatics **22**, 3067–3074 (2006).

[47]J. A. C. Gallas, "Structure of the parameter space of the Henon map," Phys. Rev. Lett. **70**, 2714–2717 (1993).

[48]J. A. C. Gallas, "Dissecting shrimps—Results for some one-dimensional physical models," Physica A **202**, 196–223 (1994).

[49]L. F. Olsen and A. Lunding, "Chaos in the peroxidase-oxidase oscillator," Chaos **31**, 013119 (2021).

[50]J. G. Freire, M. R. Gallas, and J. A. C. Gallas, "Chaos-free oscillations," Europhys. Lett. **118**, 38003 (2017).

[51]T. L. Carroll, "Dimension of reservoir computers," Chaos **30**, 013102 (2020).